EXPERIMENTAL VALIDATION OF A DYNAMIC MODEL FOR A MONO-TUBE CAVITY RECEIVER

José I. Zapata, Greg Burgess, John Pye
Research School of Engineering, Australian National University, Canberra, ACT 0200, Australia
Keywords: solar-thermal, direct steam generation, moving-boundary formulation, ANU

Abstract

This paper describes a dynamic model of a steam cavity receiver and presents results from simulations performed using this model in TRNSYS 16. The results are compared with experimental data to inform the calibration of specific model parameters. Using the experimental data obtained from the SG4 500 m² dish at the ANU, it is possible to select a set of model parameters that produce good agreement between simulated and measured receiver outlet temperatures. It is found that radiation and convection loss coefficients are consistent between experimental runs and do not require repeated calibrations. In contrast, it is found that a parameter modelling average reflectivity on the dish concentrator varies between experimental runs, due to the soiling and cleaning of the concentrator mirrors, and needs to be recalibrated in the model for each run.

Introduction

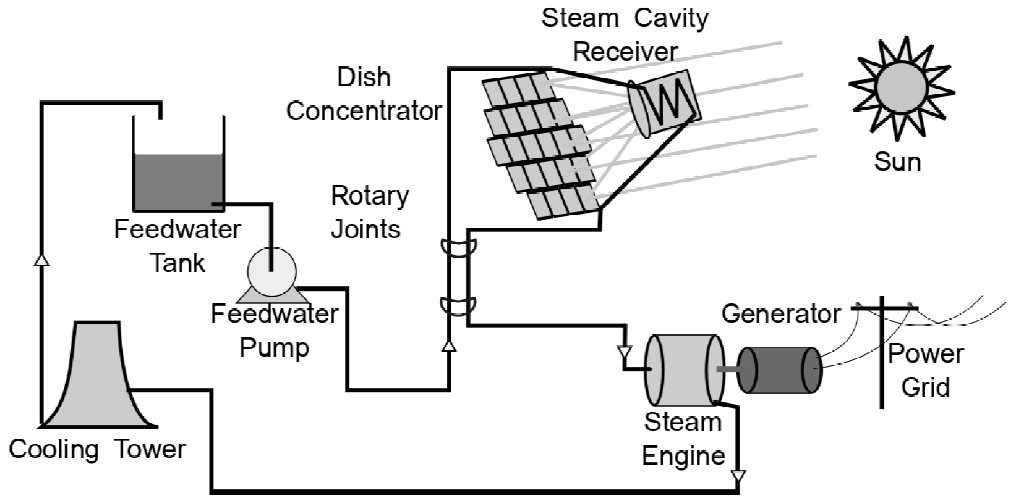

Figure 1: SG4 steam generation system at the Australian National University

The Australian National University (ANU) has been using the SG4 500 m² paraboloidal dish [1] to study direct steam generation (DSG) for power production on large scale dish arrays. The paraboloidal dish is the heat source for a mono-tube steam cavity receiver that generates superheated steam at 500 °C and 4.5 MPa in once-through mode (i.e. the fluid only passes once through the receiver and it is sent to the power block directly). A diagram of the system is shown in Figure 1.The ANU Solar Thermal Group has been working on a dynamic model of the steam cavity receiver as part of this research [2] that builds on previous studies on this topic [3]. The model is derived from first principles of mass, energy and momentum conservation in the receiver tube and uses a 'moving-boundary' approach to account for phase changes in the water [4]. This results in a compact state-space formulation of the receiver, suitable for the development of closed loop temperature control strategies [5].

In this study, the model is validated by comparing simulations of a TRNSYS implementation of the model to experimental runs of the SG4 system. The parameters of the model are calculated and adjusted, based on physical principles and experimental receiver data.

SG4 steam generation system

Components

The SG4 steam generation system in Figure 1 is configured to run a steam Rankine power cycle. The steam engine is a modified 4 cylinder Diesel engine, coupled to an induction generator that feeds power to the internal university grid. The rotary joints allow the piping of feed-water and steam return between the receiver and the power block to move with the dish as it tracks the sun in two axes.

There is process instrumentation for all system components, which is routed to a Yokogawa Supervisory Control and Data Acquisition (SCADA) system. The SCADA system interconnects Yokogawa FAM3 Programmable Logic Controller (PLC), a MW100 data acquisition system and a computer interface for monitoring and control of the system.

Data collection

The SCADA system collects measurements of pressure, temperature and other variables along the feed-water line, steam line and steam system components. The SCADA also monitors the dish tracking system, which informs of the position and status of the dish (e.g. on sun, tracking, parked, etc.).

This study uses data that relates to the operation of the receiver. The receiver is fitted with pressure sensors and thermocouples at the inlet/ outlet ports. There are additional thermocouples along the tube length. In addition, the following process data is required: feed-water mass flow, temperature and pressure measurements, direct normal irradiance (DNI) using an Eppley pyroheliometer mounted on a 2 axis tracking device, ambient temperature, and a signal that indicates if the dish is tracking or not tracking the sun.

This data is typically recorded by the SCADA system at 2 second intervals and stored in an internal database. A subset of this information, containing the measurements mentioned above, can later be extracted as plain text, which is used to simulate the receiver model.

Dynamic model of the receiver

The receiver currently installed on the SG4 500 m² dish at the ANU is formed by steel tubing arranged in a helical shape to form a cavity. The receiver tube surface inside of this cavity intercepts the concentrated radiation reflected from the SG4 dish and the other side is covered in mineral wool and a metal sheet for insulation and encasing. Water flows along a single path starting at the aperture side of the receiver and progressing into the cavity. In steady state, superheated steam exits the cavity through a port at the back of the receiver.

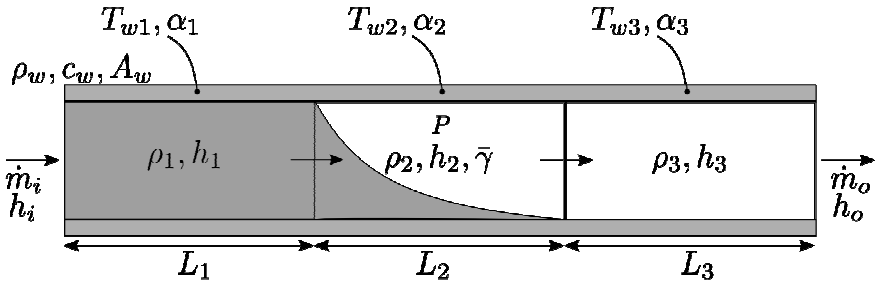

Figure 2: Dynamic receiver modelled quantities

The heat transfer processes occurring in the receiver tube are modelled by establishing mass and energy

balances for the fluid in the tube and an energy balance in the tube wall (Figure 2). The conservation equations describing the model are developed into a moving-boundary formulation of the receiver [2, 6] and switches between different moving-boundary representations of the tube using a switching approach proposed by McKinley to model evaporators and condensers in HVAC systems [7].

The model is semi-empirical. It is constructed from first principles of conservation of fluid mass, energy and momentum, but the parameters associated with the model can be selected to represent different geometries, fluids and heat transfer rates.

The model has been implemented and simulated in TRNSYS 16. The code has been implemented in FORTRAN and compiled as a TRNSYS type. The receiver parameters are input to TRNSYS type prior to the simulation and remain constant during the simulation.

At each time step, the receiver type reads data from an experimental run file (as described in the previous section) which used in the model calculations. Feed-water mass flow, temperature and pressure and receiver outlet pressure are used to calculate the balance of energy and mass in the receiver tube. Ambient temperature and DNI are used as inputs to calculate the tube wall energy balance. The dynamic change in the model is integrated numerically by the type at each time step.

Receiver model parameters

Internal heat transfer coefficients

For each fluid region in the model (i.e. liquid, saturated water/vapour and superheated steam), its properties are averaged and uniform over the region size. The wall temperature adjacent to each region is also uniform and averaged over the region length. The heat transfer between the tube and the fluid is thus governed by:

$$\alpha_n \pi D_i L_n \left(T_{wn} - T_n\right) \tag{1}$$

Where *n* is stands for the fluid region (i.e. 1 for liquid, 2 for saturated and 3 for superheated), α_n is the region forced convection coefficient; L_n is the region length, T_{wn} is the tube wall temperature and T_n the fluid temperature for the region and D_i is the internal tube diameter.

Operation temperatures for the experimental runs carried out since January 2011 on the SG4 system ranged between 400 and 550 °C and the system typically ran at approximately 500 °C. The feed-water mass flow rate required to maintain 500 °C at the receiver outlet ranged approximately between 95 and 120 g/s, depending on dish cleanliness and DNI. The knowledge of the operating conditions of the receiver was employed in an iterative calculation of heat transfer coefficients α_n.

For single phase regions, an initial guess of average region temperature, Reynolds number and other properties was taken and applied to a heat transfer correlation by Gnielinsky [8]. The resulting coefficient was applied to the model in steady state, to obtain a new temperature estimate for the region. The process was repeated until calculations converged. For the two-phase region, a heat transfer correlation by Kandlikar [9] was used instead. A summary with the results is presented in table 1.

Region	Avg. Region Temp.	Heat Transfer Coefficient	Correlation
1- Liquid	147 °C	2.5 kW/m²/K	Gnielinsky
2- Saturated	251 °C	5.6 kW/m²/K	Kandlikar
3- Superheated	365 °C	0.9 kW/m²/K	Gnielinsky

Table 1: Internal convection coefficients for receiver model

Receiver heat losses

Siangsukone [3] conducted theoretical and experimental studies to determine radiative, conductive and convective losses on the cavity receiver when it was mounted on the previous big dish, the SG3 400 m² dish. The result of these studies was the inclusion of radiative, convective and conductive losses in the cavity side of the heat balance for the receiver tube. The model in this study includes these losses in the same form.

Siangsukone calculated radiative losses to be approximately 3 kW for operating receiver outlet temperatures between 380 and 450 °C. An emissivity for steel of $\varepsilon = 0.87$ as proposed by Bannister [10] was used. The overall heat transfer coefficient in Siangsukone's data was approximately U=21 W/m²/K. This coefficient was used for typical heat losses of around 70 kW in the SG3 system. In both cases, these parameters were used in conjunction with an average cavity surface temperature that spanned the whole cavity interior. In this study, a separate view factor and overall heat transfer coefficient has been assigned for each region present in the model, to take advantage of the different tube wall temperatures calculated by the model.

The wall heat balance for each region in the model relates the dynamic changes in wall energy to the heat fluxes affecting the receiver tube. A simplified form of the balance in the model for this study is presented in equation (2).

$$\frac{dE_{wn}}{dt} = L_n\left(\frac{\dot{Q}_{dish}}{L} - G_n\varepsilon\sigma\pi D_o\left(T_{wn}^4 - T_a^4\right) - U_n\pi D_o\left(T_{wn} - T_a\right) - \alpha_n\pi D_i\left(T_{wn} - T_n\right)\right) \quad (2)$$

The first term on the left side of equation (2) is the amount of concentrated heat flux intercepted by the tube along the length of each region, assuming an even distribution over the entire tube length. The second term is the losses to ambient caused by black body radiation, where G_n is the averaged view factor for the region, ε is the surface emissivity, σ is the Stefan-Boltzmann constant and D_o is the outer tube diameter. The third term combines convective losses to the air in the cavity and conductive losses to the mineral wool insulation surrounding the receiver with the overall heat transfer coefficient U_n for each region. The fourth term is the energy transferred from the tube to the fluid, as described in the above section.

The use of separate view factors G_n and overall factor coefficients U_n takes advantage of different wall temperatures along the tube, in accordance with how the fluid changes energy as it traverses the receiver. In addition, the length and position of the fluid regions is linked to a specific area of the cavity surface. In effect the superheated region is always located at the back of the cavity, the boiling region covers a “belt” at approximately the middle of the cylindrical section of the cavity and the liquid region

spans the rest of the cavity towards the aperture of the cavity.

The model calculates approximately 80 kW of convective/conductive losses and approximately 6 kW of reflective losses when the SG4 dish average reflectivity is 85% and the receiver outlet temperature is 500 °C. These values are slightly higher than those found by Siangsukone, in part due to the higher fluxes and higher operating temperatures obtained from the SG4 experimental runs.

The calculation of accurate overall heat loss coefficient is difficult due to the ongoing challenge to accurately measure the reflectivity of the dish. A simulation of the receiver in Figure 3 shows two combinations of average reflectivity and overall heat losses that show good agreement with the measured receiver temperature.

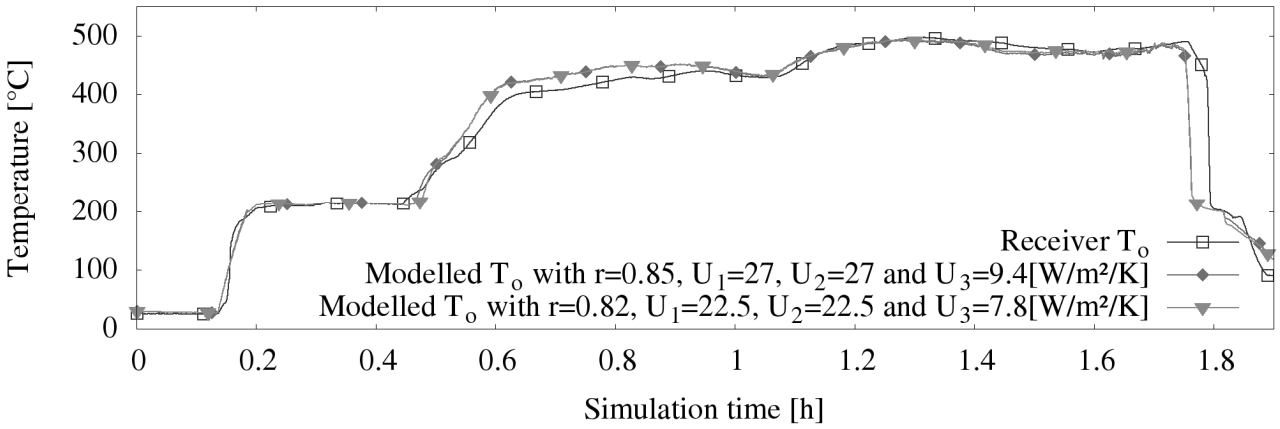

Figure 3: Measured receiver outlet temperature for experimental run on the 20th of January 2012 against two simulations with different combinations of average reflectivity and overall heat loss coefficients

This shows that if more radiation impacts the receiver (bigger *r*), greater losses restore the heat balance and the same amount of thermal energy is gained by the fluid. The lower bound for this condition is to have zero convective losses, and the upper bound is the maximum theoretical incoming radiation, limited by the reflectivity of the dish as mentioned above. Combinations of *r* and U_n above and below the values shown on Figure 3 however produce less agreement in simulations than those presented here.

The ANU Solar Thermal Group is researching methods for more accurately determining concentrator reflectivity and receiver convection losses. Results from this research will better inform the model in calculating the influence of losses in the receiver heat balance. In the interim, simulations use higher values of reflectivity and losses (e.g. r=85% in figure 3) in order to take a conservative estimate of the thermal performance of the receiver.

Dish radiation

The heat flux concentrated by the SG4 dish and intercepted by the receiver is calculated by:

$$\dot{Q}_{dish} = r\dot{I}\left(A_{dish} - A_{rec}\right) \tag{3}$$

Where *r* is the average dish reflectivity, $\dot{I}$ is DNI A_{dish} , is the dish aperture area and A_{rec} is the area of the dish obscured by the receiver and trusses. In this expression, it is assumed that all the radiation is intercepted by the receiver, and the reflectivity is used to calibrate the influence of the dish on the receiver.

Average dish reflectivity

The average reflectivity of the paraboloidal concentrator varies between experimental runs primarily due to mirror soiling. As expressed in equation (3), the reflectivity is the only parameter that affects the calculation of concentrated radiation impacting the receiver. Thus, varying this parameter in the model mimics the soiling of the dish between runs but also incorporates permanent optical imperfections in the concentrator. Preliminary estimations of this factor range between 0.82 and 0.93 for the SG4 dish when it is clean and most of its surface is free of imperfections.

This parameter has to be adjusted in the model for each experimental run of the SG4 500 m² system, in order to obtain agreement with experimental measurements. All other model parameters, including heat loss coefficients, are assumed characteristic of the receiver design and therefore not changed between simulations, so that the agreement between the model and experimental runs depends only on the adjustment of average reflectivity *r* during this process.

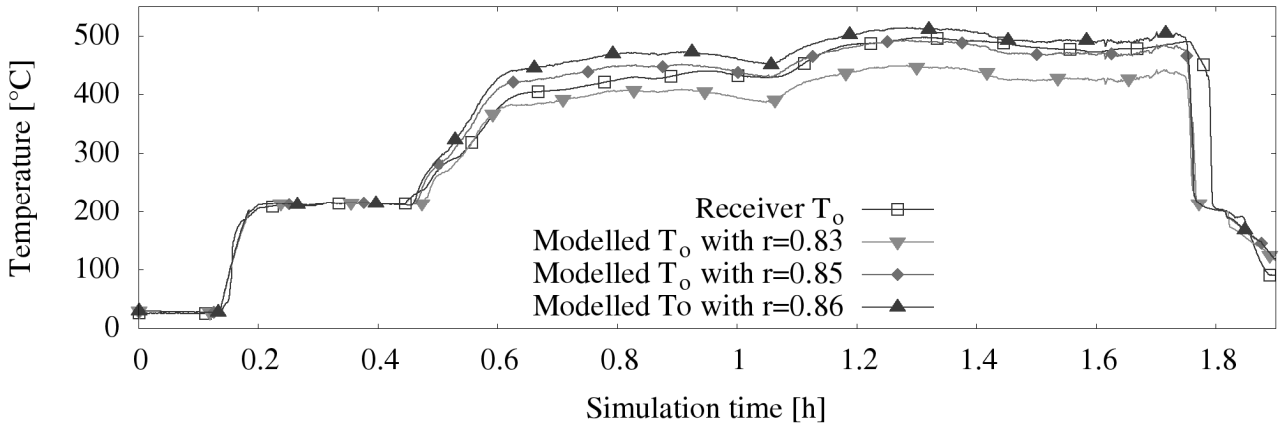

Figure 4: Measured and simulated receiver outlet temperature for experimental run on 20th January 2012 demonstrating the effect of average reflectivity and intercepted power on modelled receiver behaviour

When a new set of data is fed to the receiver model, the value of the average reflectivity is adjusted until the simulated outlet temperature agrees with the experimental run. For example, Figure 4 presents a simulation of the model with an average reflectivity *r*=85%, that achieves the closest agreement with experimental data. In addition, a simulation with two other reflectivity values of previous iterations, *r*=83% and *r*=86% has been included to show that the model sensitivity to this parameter.

The model outlet temperature is calculated from receiver average pressure P and receiver outlet enthalpy h_o. Changes in outlet enthalpy are proportional to changes in reflectivity, and the conversion from enthalpy to temperature magnifies the influence of r on T_o.

As seen in Figure 3, the modelled concentrator reflectivity may be determined by matching with experimental data for a given receiver overall heat transfer coefficient. As there have been difficulties measuring the average reflectivity of the concentrator, this remains a free-variable in the simulation.

Receiver outlet mass flow

The outlet mass flow of the receiver is calculated from outlet pressure measurements and modelled fluid quantities by expression (4) (derivation details of which can be found in [6])

$$\dot{m}_o = \sqrt{\dot{m}_i^2 + 2(P - P_o)A^2\overline{\rho} - \tau\pi A\overline{\rho}D_i L}$$
$$\dot{m}_o = \sqrt{\dot{m}_i^2 + k_m(2(P - P_o)A^2\overline{\rho} - \tau\pi A\overline{\rho}D_i L)} \quad (4)$$

The shear stress coefficient τ in (4) is calibrated to account for pressure drops on the receiver and k_m is a damping factor for when the receiver model is in superheated outlet mode. The pressure difference between P and P_o balances against the shear force produced by the inner surface of the tube when the receiver model is in equilibrium. The term $2(P - P_o)$ can be linked to the pressure drop in the tube if the pressure drop is considered linear and the receiver modelled pressure is the average of the two so that

$$P = \frac{P_i + P_o}{2} \quad (5)$$

Therefore, the shear stress coefficient can be calculated as:

$$\tau = \frac{(P_i - P_o)A}{\pi D_i L} \quad (6)$$

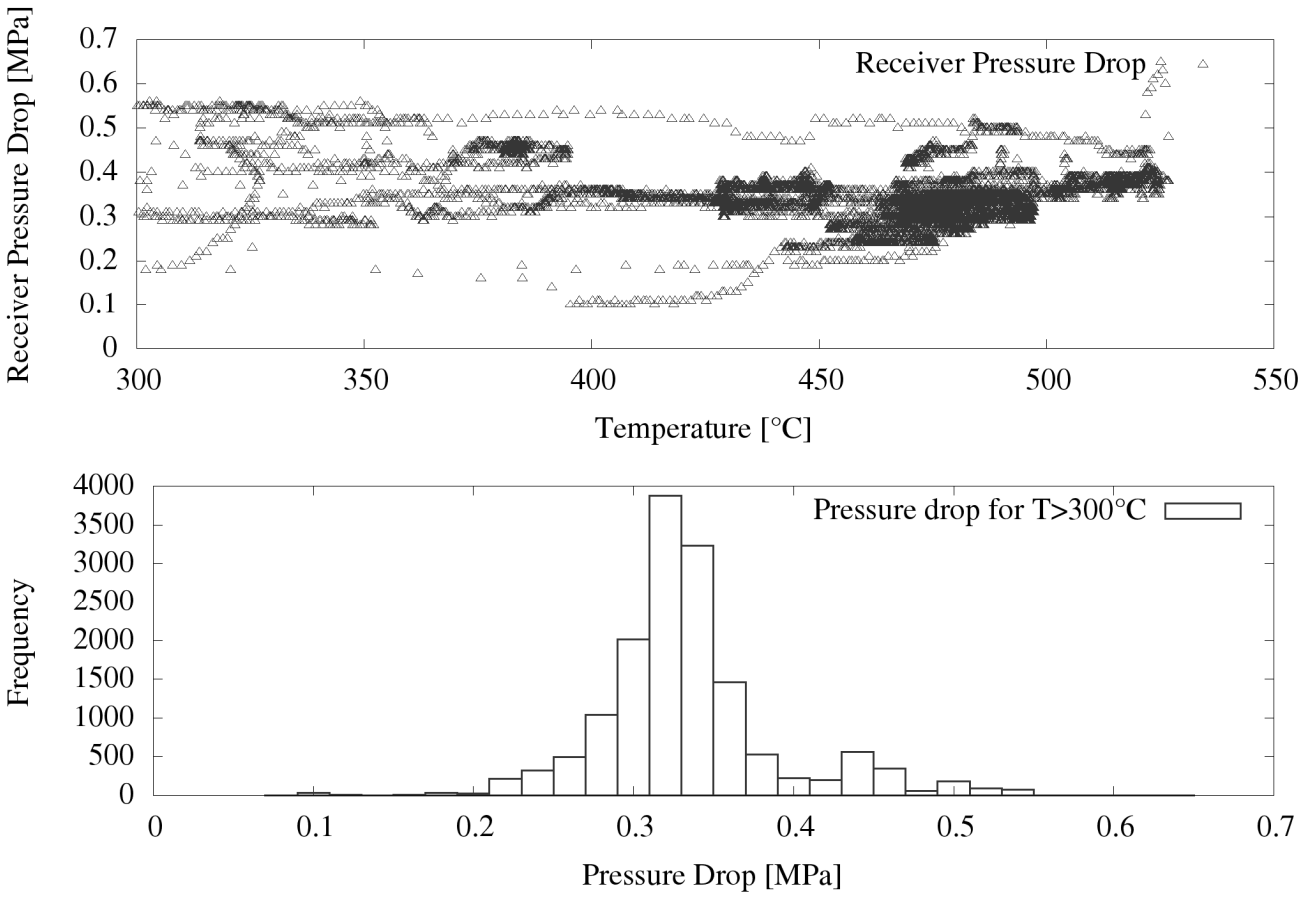

Figure 5: Receiver pressure drop vs outlet temperature samples for 3 experimental runs (above). Frequency distribution of pressure drops (below)

The difference between recorded inlet and outlet pressures for every data point over 3 different experimental runs has been plotted against receiver temperature in Figure 5. In order to separate transient effects from steady state operation of the receiver, only data points for temperatures above 300

°C have been included. Start-up periods and the passage of large clouds involve transients where the receiver outlet transitions from liquid to saturated flow and from saturated to superheated flow. Measurements of pressure drop in the receiver for temperatures over 300°C ensure that the receiver outlet is superheated and therefore the flow pattern described by the receiver model has been established. In addition, Figure 5 shows a histogram of pressure drop measurements in 0.1 MPa intervals to count the frequency for measurements above 300 °C.

Based on these measurements, the typical pressure drop in the receiver is considered to be 0.31 MPa, which results in a shear stress coefficient of 7.31x10-3 kPa.

Future work

The calculation of average dish reflectivity *r* will be refined by the acquisition of an industry standard reflectometer and the detailed measurement of reflectivity across the SG4 dish surface. Additional steam generation system runs over successive days will contribute to characterise the changes in average reflectivity due to soiling.

Numerical and experimental studies of the convective heat losses on the cavity receiver will also improve the calculation of the overall heat transfer coefficient *U*.

Both these efforts will allow the model to produce a more accurate heat balance of the receiver for static calculations and improve the response of a temperature controller to changes in mirror reflectivity and heat losses.

Conclusion

A dynamic model for simulating two-phase flow in a steam solar receiver was presented. Experimental results exhibiting the dynamic temperature and pressure from the ANU SG4 dish receiver were compared with simulation results and good agreement was found, subject to necessary adjustments of some unknown parameters. Future experiments on receiver efficiency and concentrator reflectivity will further enable realistic simulations with this model, from which more insight into the dynamic behaviour of two-phase flows in solar-thermal receivers can be extracted.

References

[1] K. Lovegrove, G. Burgess and J. Pye, 2011. 'A new 500 m2 paraboloidal dish solar concentrator', *Solar Energy* **85**, 620 - 626.

[2] J. Zapata, J. Pye and K. Lovegrove, 2011. 'Dynamic Simulation of Mono-tube Cavity Receivers for Direct Steam Generation'. In *SolarPACES 2011 conference, Granada, Spain.*

[3] P. L. Siangsukone, 2005. 'Transient Simulation and Modeling of a Dish Cavity Receiver', PhD thesis, Australian National University.

[4] J. Jensen and H. Tummescheit, 2002. 'Moving Boundary Models for Dynamic Simulations of Two-Phase Flows'. In *Proc. of the 2nd Int. Modelica Conference*.

[5] X.-D. He, S. Liu, H. H. Asada and H. Itoh, 1999. 'Multivariable control of vapor compression systems', *ASHRAE Transactions 105*.

[6] J. Zapata, J. Pye and G. Burgess, 2012. 'Estimation of outlet mass flow for a mono-tube cavity receiver for direct steam generation'. In *Proceedings of the SolarPACES conference, Marrakech, Morocco* .

[7] T. L. McKinley and A. G. Alleyne, 2008. 'An advanced nonlinear switched heat exchanger model for vapor compression cycles using the moving-boundary method', *International Journal of Refrigeration* **31**, 1253 - 1264.

[8] V. Gnielinski, 1976. 'New equations for heat and mass transfer in turbulent pipe and channel flow', *Int. Chem. Eng* **16**, 359-368.

[9] S. G. Kandlikar, 1990. 'A General Correlation for Saturated Two-Phase Flow Boiling Heat Transfer Inside Horizontal and Vertical Tubes', *Journal of Heat Transfer* **112**, 219-228.

[10] P. Bannister, 1991. 'An experimental and analytical assessment of a steam rankine solar thermal system', PhD thesis, Australian National University.

Contact author: José Zapata – jose.zapata@anu.edu.au